Electrochimica Acta 55 (2010) 2472–2476

Contents lists available at ScienceDirect

Electrochimica Acta

journal homepage: www.elsevier.com/locate/electacta

Synthesis of tellurium nanotubes by galvanic displacement

Youngwoo Rheem[a], Chong Hyun Chang[a], Carlos M. Hangarter[a], Deok-Yong Park[b], Kyu-Hwan Lee[c], Yong-Soo Jeong[c], Nosang V. Myung[a,*]

[a] Department of Chemical and Environmental Engineering, University of California-Riverside, Riverside, CA 92521, United States
[b] Department of Applied Materials Engineering, Hanbat National University, Daejon 305-719, Republic of Korea
[c] Electrochemical Processing Group, Korea Institute of Materials Science, Changwon-Si, Kyungnam 641-010, Republic of Korea

ARTICLE INFO

Article history:
Received 24 October 2009
Received in revised form 1 December 2009
Accepted 3 December 2009
Available online 5 December 2009

Keywords:
Tellurium
Nanotube
Galvanic displacement
Thermoelectrics
Magnetoresistance

ABSTRACT

Tellurium nanotubes with controlled diameter and wall thickness were synthesized by galvanic displacement of cobalt nanowires and their temperature dependent field effect transistor and magnetoresistance properties were systematically investigated. The nanotube diameter was slightly larger than the sacrificial cobalt nanowire diameter with a wall thickness of range from 15 to 30 nm depending on the diameter of cobalt nanowires. Te nanotubes show p-type semiconducting property with the field effect carrier mobility of approx. 0.01 $cm^2/V\,s$ which is relatively lower than other 1D nanostructure. Low mobility might be attributed to porous morphology with small grain size (<10 nm). Temperature dependent mobility also exhibiting a Conwell–Weisskopf relationship to temperatures below 250 K, indicating that the dominant scattering sites are ionized impurity centers. Unique MR behavior was observed from nanotube with a maximum magnetoresistance ratio of 37% at 260 K.

1. Introduction

Tellurium is a p-type semiconductor with a direct band gap energy of 0.35 eV at room temperature. It has been applied for high-efficiency photoconductors [1], piezoelectric devices [2], and carbon monoxide [3] and ammonia [4] gas sensors. Additionally, tellurium and its alloys are considered important semiconductor materials for thermoelectric generators and coolers because of their high thermopower [5]. Unfortunately, the thermoelectric figure of merit of pure bulk tellurium is relatively low because of its high thermal conductivity. However, one-dimensional (1D) nanostructures have been proposed to increase the thermoelectric figure of merit by decreasing thermal conductivity via phonon scattering. Thus, the synthesis of one-dimensional tellurium nanostructures is of great interest. Furthermore, Te nanotubes, in particular, are attractive 1D nanostructures as their wall thickness allows their physical properties to be tuned by much smaller characteristic lengths compared to their diameter.

Previous reports have synthesized Te nanotubes via hydro-/solvo-thermal [6,7] and physical vapor deposition [8]. However, these processes are limited by low yield (<30%) and inability to produce high aspect ratio nanotubes, which is essential for nanostructure-based thermoelectric devices. Alternatively, galvanic displacement reactions, which are induced by the difference in redox potentials between materials, are site-specific electrochemical processes producing structural features determined by those of the sacrificial material. Galvanic displacement reaction is simple and versatile route to create nanostructures with controllable hollow interiors and porous walls. The requirement for achieving such hollow nanostructures is the availability of noble metal ions in the presence of less-noble nanoconstructures. Various hollow metal nanostructures including nanocubes and nanotubes have been synthesized via this reaction [9]. Recently, we demonstrated the synthesis of semiconducting nanostructures using galvanic displacement [10].

In this work, Te nanotubes with controlled diameters and wall thickness were systematically synthesized by galvanic displacement of sacrificial cobalt nanowires. The nanotube diameter was adjusted by the diameter of the sacrificial nanowires. Temperature dependent electron- and magneto-transport properties of single tellurium nanotube were also investigated.

2. Experiments

The sacrificial cobalt nanowires with average diameters of 70, 120 and 220 nm were synthesized by a template-directed electrodeposition method using polycarbonate membranes as scaffolds. A gold thin film with a thickness of 200 nm was deposited on one side of the template with an Emitech K550 table-top sputter to serve as the seed layer for the electrodeposition of

* Corresponding author. Tel.: +1 951 827 7710; fax: +1 951 827 5696.
E-mail address: myung@engr.ucr.edu (N.V. Myung).

0013-4686/$ – see front matter © 2009 Elsevier Ltd. All rights reserved.
doi:10.1016/j.electacta.2009.12.002

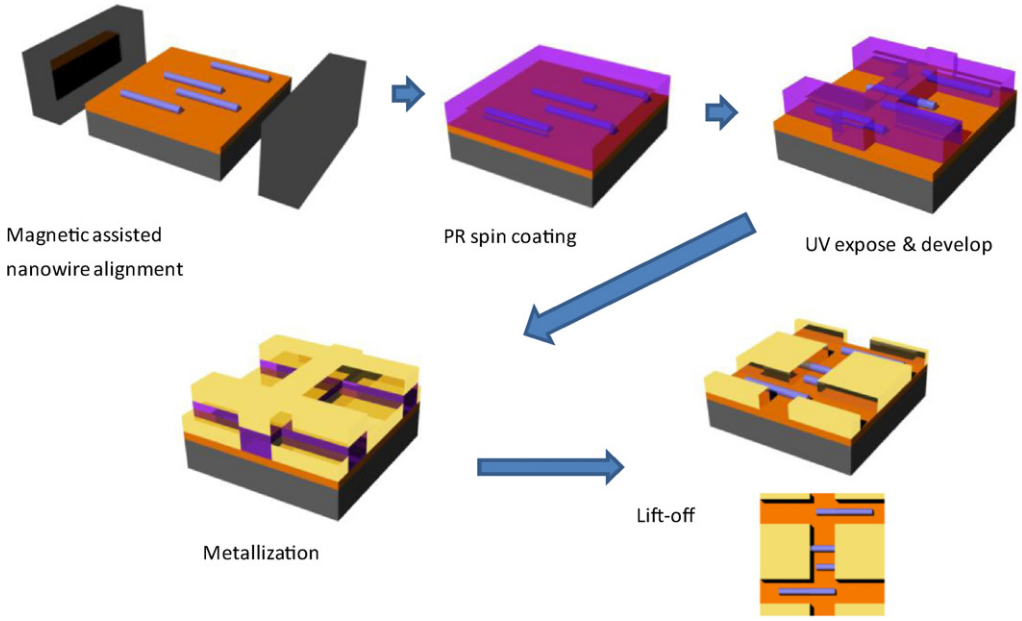

Fig. 1. Schematic representation of fabrication procedure to create top areal electrode contact on nanowires.

cobalt nanowires. The nanowires were galvanostatically deposited by applying current density of 5 mA/cm^2 using EG&G PAR VMP2 multi-channel potentio/galvanostat. The cobalt electrolyte consisted of 1 M $CoCl_2$ + 1 M $CaCl_2$ at pH of 3. After electrodeposition, the nanowires were released in isopropyl alcohol by dissolving the template in 1-methyl-2-pyrrolidinone. Tellurium nanotubes were synthesized by galvanically displacing the cobalt nanowires. The galvanic displacement electrolyte (0.01 M $HTeO_2^+$ + 1 M HNO_3, pH of 1) for the tellurium nanotubes was prepared by dissolving TeO_2 in concentrated nitric acid followed by addition of deionized water to reach the final volume.

Electron- and magneto-transport characterization of single tellurium nanotubes required a back gated two-point electrical contact configuration. To create a robust electrical and mechanical contact between nanowire and microfabricated electrodes, device fabrication began by dispersing suspended cobalt nanowires (average diameter of 220 nm) on a boron doped silicon substrate (ρ = 0.01–0.02 Ω cm) coated with a HfO_2 dielectric layer (150 nm thickness). After assembly of nanowires, Au/Cr electrodes (200 μm × 200 μm, t_{Au} = 280 nm, t_{Cr} = 20 nm) with 3 μm gap were fabricated on top of the nanowires by e-beam evaporation and standard lift-off lithography (Fig. 1). Substrates with contacted cobalt nanowires were immersed in the tellurium electrolyte to form tellurium nanotubes. The reaction was carried out with no agitation at ambient temperature and a fixed time of 30 min. The temperature dependence of electro- and magneto-transport properties of single tellurium nanotube were measured using a source-measure-unit (Keithley 2636) and a physical property measurement system (PPMS, Quantum Design), respectively.

3. Results and discussion

Fig. 2 shows the transmission electron microscopy (TEM) image of electrodeposited cobalt nanowires with average diameters of 70 nm and tellurium nanotubes subsequently synthesized from these wire by galvanic displacement. Selected area electron diffraction (SAED) pattern of the nanowires indicates a nanocrystalline microstructure (Fig. 2(a)). When cobalt nanowires are immersed into the acidic nitric solution containing $HTeO_2^+$ ions, cobalt nanowires are galvanically displaced

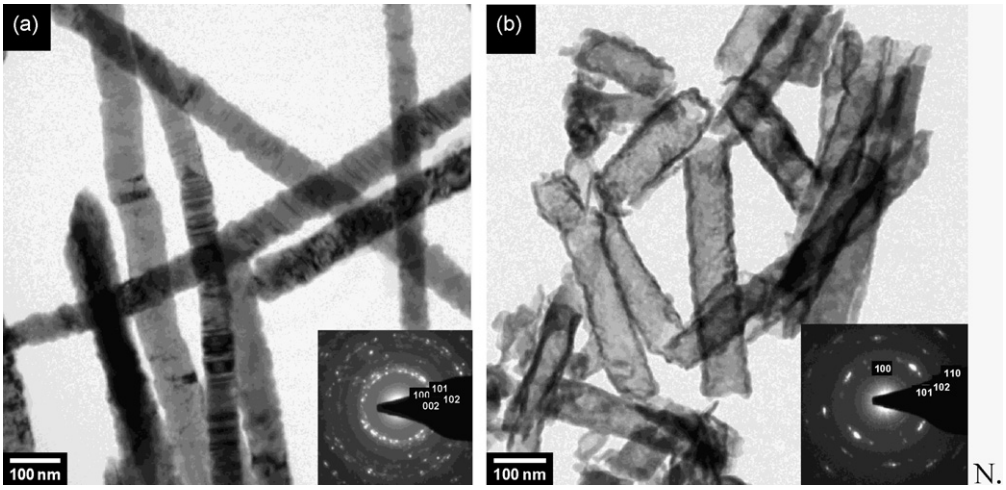

Fig. 2. TEM images and selected area electron diffraction patterns of (a) electrodeposited cobalt nanowires and (b) tellurium nanotubes.

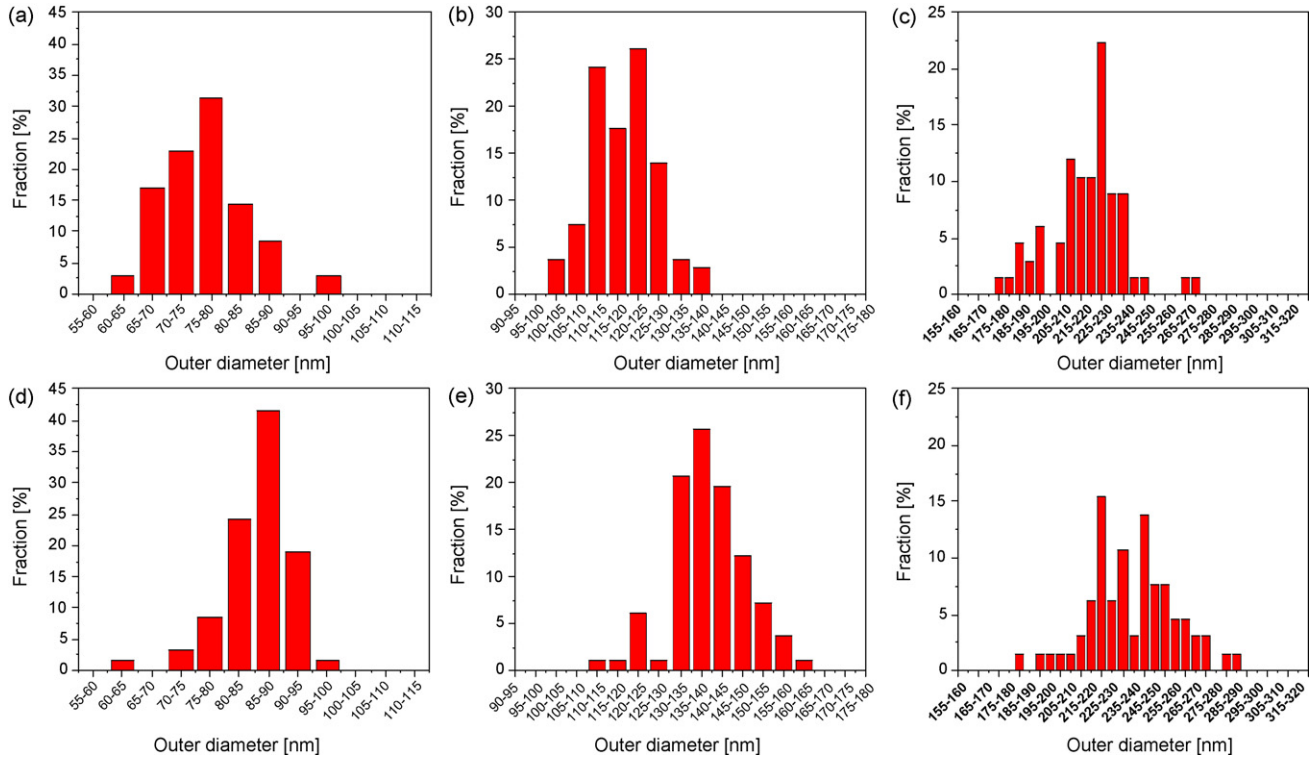

Fig. 3. Outer diameter distribution of Co nanowires (a–c) and Te nanotubes (d–f). The mean diameter of Co nanowires are (a) 70, (b) 120, and (c) 220 nm, respectively.

to form tellurium, because of the difference in the redox potentials (*i.e.*, $Co^{2+} + 2e^- \rightarrow Co$ ($E^0 = -0.28$ V vs NHE) and $HTeO_2^+ + 3H^+ + 4e^- \rightarrow Te + 2H_2O$ ($E^0 = +0.551$ V vs NHE)) [11], where the galvanic displacement of cobalt nanowires to tellurium nanotubes can be represented as follows:

$$HTeO_2^+(aq) + 3H^+(aq) + 2Co^0(s) \rightarrow Te^0(s) + 2H_2O + 2Co^{2+} \quad (1)$$

Homogeneous tellurium nanotubes with well-defined void spaces were formed as shown in Fig. 2(b) where the SAED pattern also confirms the formation of tellurium nanotubes. The final outer diameter of the tellurium nanotubes was slightly larger than the cobalt nanowires. These results are in accord with the proposed mechanism for tube formation, in which the displacement reaction occurs at the surface of the nanowire creating an incomplete thin tellurium sheath at the cobalt nanowire surface. The reactants and products diffuse across the porous tellurium sheath, building a continuous tellurium nanotube on the exterior wall of the initial tellurium sheath. The tellurium nanotubes also have a nanocrystalline microstructure with a grain size <10 nm and wall thickness around 15 nm which was measured using TEM images. The nanocrystalline microstructure of the Te nanotube implies the crystallinity of the sacrificial Co nanowire may be induced upon the Te nanotube during the displacement reaction. Fig. 3 shows the histogram of outer diameter distribution of sacrificial cobalt nanowires and tellurium nanotubes where the average diameter of the Te nanotubes were determined to be 85, 140, and 250 nm for sacrificial cobalt nanowires diameters of 70, 120 and 220 nm, respectively. As expected, the outer diameter of Te nanotubes was greater than the diameter of sacrificial cobalt nanowire. In addition, the wall thickness increased from 15, 20 and 30 nm which increased in the diameter of cobalt nanowires from 70, 120, and 220 nm. These clearly indicated that the tube diameter and wall thickness can be tuned by adjusting the diameter of sacrificial nanowires.

To determine the thermal activation energy of synthesized Te nanotubes, temperature dependent electrical resistance were measured from 20 to 300 K. Fig. 4(a) shows the Arrhenius plot of temperature dependent resistance of a single tellurium nanotube (220 nm in diameter). Two linear regions are observed with activation energies of 87 and 6.8 meV obtained for temperatures above and below 200 K. These values fall within the range of activation energies, between 6 and 178 meV, reported by Goswami and Ojha [12] for thermally evaporated tellurium thin films with variation in film thickness and fabrication conditions. The transition temperature (200 K) of tellurium nanotubes is also similar to that of tellurium thin films.

To determine semiconducting properties of single Te nanotubes, field effect transistor (FET) transfer characteristics were measured. Fig. 4(b) shows a series of the source-drain current (I_{SD}) versus voltage (V_{SD}) curves measured at different gate voltage (V_G) from −20 to +20 V with a step of 10 V under ambient condition. The back gate was formed by contacting highly doped silicon substrate back-side with metal electrode using conductive silver paint (PELCO Conductive Silver 187). The I_{SD}–V_{SD} curves at different V_G are all linear, which indicate ohmic contact between gold electrodes and Te nanotube. The dependence of I_{SD}–V_{SD} on the V_G indicates that the synthesized tellurium nanotube is a p-type semiconductor. The transfer characteristics of the tellurium nanotube are shown in Fig. 4(c) with fixed V_{DS} of 1 V. The conductance of the tellurium nanotube decreased with the increase in V_G indicating the tellurium nanotube has typical characteristics of a p-channel semiconductor field effect transistor (FET). In addition, we investigated the carrier mobilities at temperatures from 50 to 300 K using a cold-finger cryogenic system (Janis CCS-350SH). The mobility of the carriers can be estimated from the transconductance of the FET, $dI_{SD}/dV_G = \mu(C/L^2)V_{SD}$, where μ is the carrier mobility. The approximate nanotube capacitance $C = 2\pi\varepsilon\varepsilon_0 L/\ln(2h/r)$, where ε is dielectric constant of HfO_2, h is the thickness of the HfO_2 layer, L is the nanotube length, and r is radius of tellurium nanotube [13]. The temperature dependence of carrier mobility of tellurium nanotube

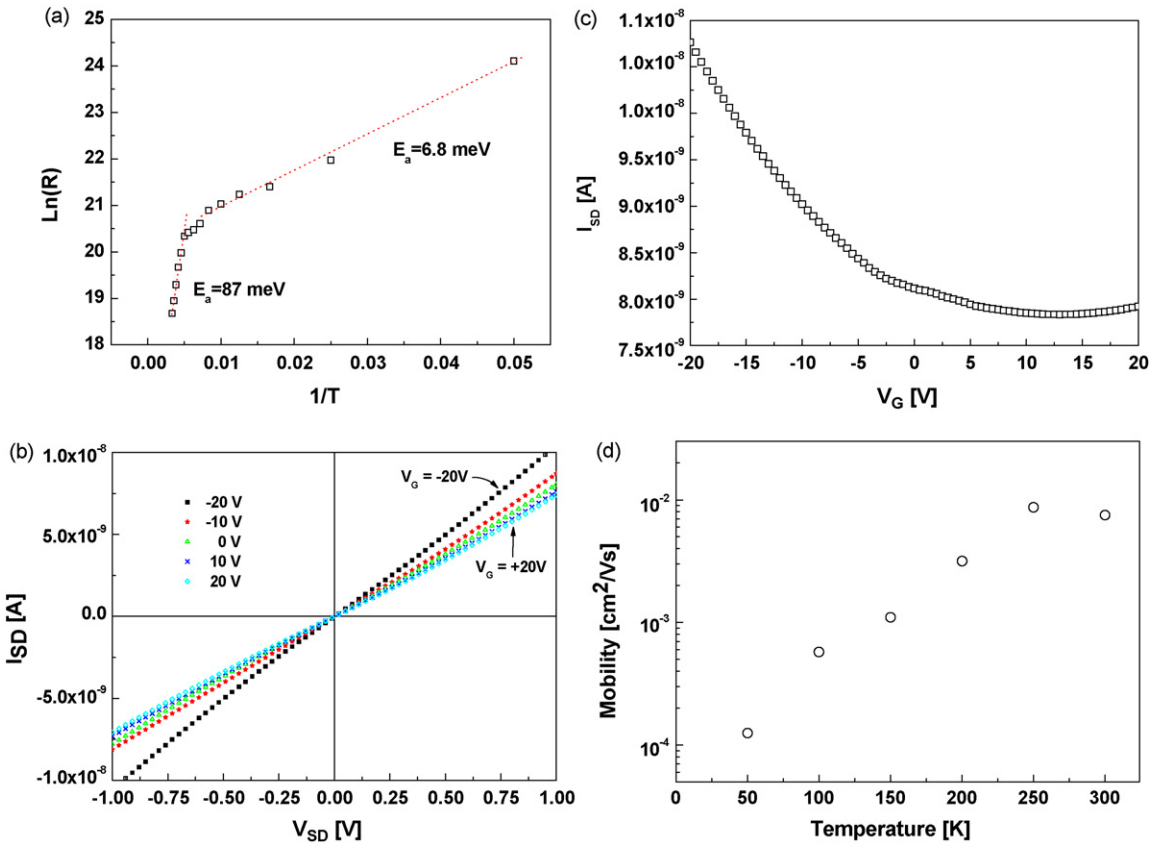

Fig. 4. Electron transport properties of tellurium nanotube device; (a) temperature dependence of electrical resistance, (b) the gate voltage dependent I_{SD}–V_{SD} curves, (c) I_{SD}–V_G characteristics measured at V_{SD} = 1 V, and (d) temperature dependence of field effect carrier mobility.

(Fig. 4(d)) shows that the field effect carrier mobility monotonically increased with increase in temperature up to 250 K, and slightly decreased with further increases in temperature. The field effect mobility at 300 K was approx. 0.01 $cm^2/V\,s$ which is relatively lower than other reported semiconducting nanostructures. For example, field effect mobility of single-walled carbon nanotubes network is in the range of 0.1–10 $cm^2/V\,s$ [14]. The lower mobility might be attributed to porous morphology of Te nanotubes with small grain size. The field effect carrier mobility below 250 K seems to obey the Conwell–Weisskopf relation [15], indicating that ionized impurity center scattering is the dominant factor in this region [16]. In the temperature region above 250 K, the mobility is affected by lattice scattering mode following $T^{-3/2}$ law. The field effect carrier mobility was estimated based on transconductance.

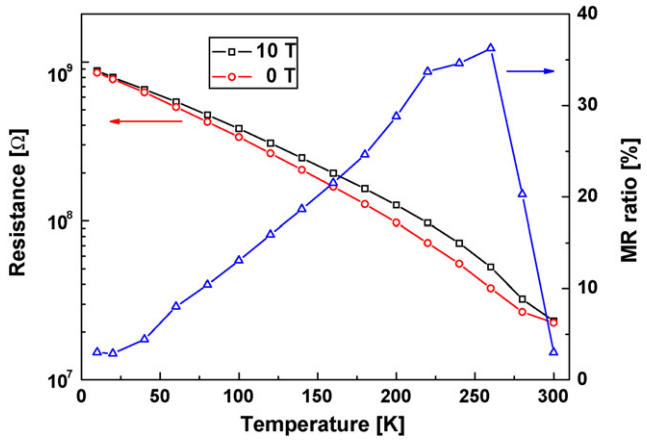

Fig. 5. Temperature dependence of resistance of tellurium nanotube device in the absence and presence of external magnetic field (H = 10 T) in the transverse direction. The triangle symbol shows the temperature dependence of the magnetoresistance ratio of the nanotube device.

Magnetoresistance (MR) properties of tellurium nanotube in the temperature range from 10 to 300 K were measured using a PPMS with a two-probe contact. The temperature dependence of resistance with zero magnetic field and applied field of H = 10 T, and MR ratio are shown in Fig. 5. The magnetic field was applied in the transverse direction. The resistance curves show the ordinary semiconductor properties with higher resistance under an applied magnetic field at all temperatures. The MR ratio has maximum value of 37% at 260 K and decreases gradually with decreasing temperature. It is known that the transverse magnetoresistance of the medium with one kind of carrier increases with magnetic field as $(\mu H)^2$ relation, where μ and H are the carrier mobility and magnetic field strength, respectively [17]. However, the MR mechanism of tellurium is not clear at this moment [18–20].

4. Conclusion

For the first time, we reported the synthesis of Te nanotubes with controlled diameter and wall thickness from sacrificial Co nanowires by galvanic displacement reaction at room temperature. The diameter and wall thickness of the nanotubes were controlled by adjusting the diameter of the sacrificial nanowires. The length can be also controlled by adjusting the length of sacrificial nanotube. As expected, the diameter and wall thickness of nanotube increased with increases in the diameter of cobalt nanowires. As-synthesized Te nanotubes show nanocrystalline microstructure with an average grain size below 10 nm. The wall thickness of nanotubes ranged from 15 to 30 nm depending on the diameter of cobalt nanowire. Synthesized nanotubes show typical p-type

semiconductor with field effect mobility of approx. 0.01 $cm^2/V s$. In addition, unique MR behavior was observed from single Te nanotube.

Acknowledgement

The work was supported by Korea Foundation for International Cooperation of Science and Technology (KICOS) through a grant provided by the Korean Ministry Science and Technology (MOST) in K207010000284-07A0100.

References

[1] Y. Wang, Z. Tang, P. Podsiadlo, Y. Elkasabi, J. Lahann, N. Kotov, Advanced Materials 18 (2006) 518.
[2] S. Fukuda, T. Shiosaki, A. Kawabata, Ultrasonics Symposium (1979) 9.
[3] D. Tsiulyanu, S. Marian, H.D. Liess, Sensors and Actuators B: Chemical 85 (2002) 232.
[4] S. Sen, K.P. Muthe, N. Joshi, S.C. Gadkari, S.K. Gupta, Jagannath, M. Roy, S.K. Deshpande, J.V. Yakhmi, Sensors and Actuators B: Chemical 98 (2004) 154.
[5] P. Bodiul, N. Bondarchuk, T. Huber, L. Konopko, A. Nikolaeva, O. Botnari, 25th International Conference on Thermoelectrics (2006) 607.
[6] G. Xi, Y. Peng, W. Yu, Y. Qian, Crystal Growth and Design 5 (2005) 325.
[7] H. Zhang, D. Yang, X. Ma, D. Que, Journal of Crystal Growth 289 (2006) 568.
[8] S. Sen, U.M. Bhatta, V. Kumar, K.P. Muthe, S. Bhattacharya, S.K. Gupta, J.V. Yakhmi, Crystal Growth and Design 8 (2008) 238.
[9] X. Lu, J. Chen, S.E. Skrabalak, Y. Xia, Proceedings of the Institution of Mechanical Engineers, Part N: Journal of Nanoengineering and Nanosystems 221 (2007) 1.
[10] F. Xiao, B. Yoo, K.H. Lee, N.V. Myung, Journal of the American Chemical Society 129 (2007) 10068.
[11] D.R. Linde, W.M. Haynes, CRC Handbook of Chemistry & Physics, CRC Press, Cleveland, OH, 2006.
[12] A. Goswami, S.M. Ojha, Thin Solid Films 16 (1973) 187.
[13] R. Martel, T. Schmidt, H.R. Shea, T. Hertel, P. Avouris, Applied Physics Letters 73 (1998) 2447.
[14] J.H. Lim, N. Phiboolsirichit, S. Mubeen, M.A. Deshusses, A. Mulchandani, N.V. Myung, Electroanalysis, Epub ahead of print.
[15] E. Conwell, V.F. Weisskopf, Physical Review 77 (1950) 388.
[16] R.W. Dutton, R.S. Muller, Proceedings of the IEEE 59 (1971) 1511.
[17] J.L. Olsen, Electron Transport in Metals, Interscience Publishers a division of John Wiley & Sons, New York, London, 1962.
[18] C. Albers, H. Gertig, Physica Status Solidi (a) 34 (1976) K125.
[19] X.-L. Li, G.-H. Cao, C.-M. Feng, Y.-D. Li, Journal of Materials Chemistry 14 (2004) 244.
[20] K. Takita, K. Suzuki, S. Tanaka, Journal of the Physical Society of Japan 34 (1973) 677.